DOI: 10.1002/mgg3.2122

ORIGINAL ARTICLE

Molecular Genetics & Genomic Medicine Open Access WILEY

Clinical features and molecular characterization of Chinese patients with *FKBP10* variants

Zhijia Tan[1,2] | **Hiu Tung Shek**[1] | **Peikai Chen**[1,2] | **Zhongxin Dong**[1] | **Yapeng Zhou**[1] | **Shijie Yin**[1] | **Anmei Qiu**[1] | **Lina Dong**[1] | **Bo Gao**[1,2] | **Michael Kai Tsun To**[1,2]

[1]Department of Orthopaedics and Traumatology, The University of Hong Kong-Shenzhen Hospital, Shenzhen, China

[2]Department of Orthopaedics and Traumatology, Li Ka Shing Faculty of Medicine, The University of Hong Kong, Pok Fu Lam, Hong Kong

Correspondence
Michael Kai Tsun To, Department of Orthopaedics and Traumatology, The University of Hong Kong-Shenzhen Hospital, Shenzhen, China.
Email: duqj@hku-szh.org

Funding information
Shenzhen "Key Medical Discipline Construction Fund", Grant/Award Number: SZXK077; Guangdong Provincial Basic and Applied Research Fund, Grant/Award Number: 2022A1515010987; Shenzhen Sanming Project, Grant/Award Number: SZSM201612055; Hong Kong Health and Medical Research Fund, Grant/Award Number: 07181676; Shenzhen Peacock Plan, Grant/Award Number: 20210830100C and 20210802658C

Abstract

Background: Osteogenesis imperfecta (OI) is a group of rare skeletal dysplasia. Long bone deformity and scoliosis are often associated with progressively deforming types of OI. FKBP65 (encoded by *FKBP10*, OMIM *607063) plays a crucial role in the processing of type I procollagen. Autosomal recessive variants in *FKBP10* result in type XI osteogenesis imperfecta.

Methods: Patients diagnosed with OI were recruited for a genetic test. RT-PCR and Sanger sequencing were applied to confirm the splicing defect in *FKBP10* mRNA with the splice-site variant. The bone structure was characterized by Goldner's trichrome staining. Bioinformatic analyses of bulk RNA sequencing data were performed to examine the effect of the *FKBP10* variant on gene expression.

Results: Here we reported three children from a consanguineous family harboured a homozygous splice-site variant (c.918-3C > G) in *FKBP10* intron and developed long bone deformity and early onset of scoliosis. We also observed frequent long bone fractures and spinal deformity in another 3 OI patients with different *FKBP10* variants. The homozygous splicing variant identified in the fifth intron of *FKBP10* (c.918-3C > G) led to abnormal RNA processing and loss of FKBP65 protein and consequently resulted in aberrant collagen alignment and porous bone morphology. Analysis of transcriptomic data indicated that genes involved in protein processing and osteoblast differentiation were significantly affected in the patient-derived osteoblasts.

Conclusion: Our study characterized the clinical features of OI patients with *FKBP10* variants and revealed the pathogenesis of the c.918-3C > G variant. The molecular analyses helped to gain insight into the deleterious effects of *FKBP10* variants on collagen processing and osteoblast differentiation.

KEYWORDS
FKBP10, genetics, osteogenesis imperfecta

Zhijia Tan and Hiu Tung Shek contributed equally to this work.

1 | INTRODUCTION

Osteogenesis imperfecta (OI), also known as brittle bone disease, is a group of rare genetic disorders that affect around 1 in 15,000 people worldwide (Forlino et al., 2011). Although the genotypes and phenotypes vary, patients with OI are generally more susceptible to long bone fractures and deformities due to low bone mass and bone brittleness. Other typical manifestations include blue sclerae, hearing loss, scoliosis and dentinogenesis imperfecta (Marini et al., 2017). Autosomal dominant variants in type I collagen encoding genes, *COL1A1* and *COL1A2*, were identified as the most prevalent disease-causing variants (Forlino et al., 2011). Since then, more than 19 OI causative genes have been identified, influencing bone mineralization, collagen post-translational modification and osteoblast differentiation (Marini et al., 2017; Moosa et al., 2019; van Dijk et al., 2020).

FKBP65 is a peptidyl-prolyl cis-trans isomerase (PPIase) acting to prevent premature aggregation of type I procollagen triple helix, together with HSP47 (heat shock protein 47) (Ishikawa et al., 2008; Satoh et al., 1996). Autosomal recessive variants in *FKBP10* result in OI type XI, Bruck Syndrome type I (represented by congenital joint contracture in addition to bone fragility) and Kuskokwim syndrome (rare disorder of joint contractures with mild skeletal defect) (Alanay et al., 2010; Barnes et al., 2013; Kelley et al., 2011). Defects in FKBP65 lead to delayed type I procollagen secretion and accumulation in the ER (Alanay et al., 2010). The quantity of collagen fibres is normally not affected in patients with OI type XI, but rather the structural arrangement and hence the quality of bone (Lietman et al., 2017). As compared with other OI sub-types, type XI patients are less likely to encounter dentinogenesis imperfecta, hearing impairment and blue sclera, but progressive scoliosis and kyphoscoliosis are usually observed (Alanay et al., 2010; Kelley et al., 2011).

In the genetic screening of a Chinese cohort ($n = 187$) diagnosed with OI (Chen et al., 2022), we identified six patients from four families harbouring pathogenic variants in *FKBP10*. All six patients (three children and three adults) displayed typical OI symptoms (low bone density and limb fractures) and spinal deformity. It is noteworthy that the three children from a consanguineous family developed early onset of scoliosis before 3 y/o. In this family, we identified a previously-described variant in the fifth intron of *FKBP10* (c.918-3C > G) without a detailed mechanistic study (Li et al., 2020; Xu et al., 2017). This splice-site variant resulted in intron retention and exon skipping, leading to the loss of FKBP65 activity. FKBP65 loss-of-function caused aberrant collagen alignment and porous bone structure. Analyses of transcriptomic data indicated that protein processing in the endoplasmic reticulum (ER) and osteoblast differentiation was significantly affected in the patients. These data suggested FKBP65 is an important regulator of the collagen process and osteoblast differentiation.

2 | MATERIALS AND METHODS

2.1 | Targeted amplicon sequencing

DNA isolated from peripheral blood was subjected to targeted amplicon sequencing (Bybee et al., 2011). Nineteen OI causative genes (including *COL1A1, COL1A2, IFITM5, SERPINF1, CRTAP, P3H1, PPIB, SERPINH1, FKBP10, BMP1, SP7, TMEM38B, WNT1, CREB3L1, SPARC, TENT5A, MBTPS2, MESD, KDELR2*) and 5 OI-related genes (*PLOD2, P4HB, SEC24D, PLS3, LRP5*) were included in the targeted sequencing panel. Libraries were prepared by a two-stage PCR process and incorporated with a unique 8-bp index for sample-specific barcoding, allowing all samples to be mixed for library purification and sequencing in a single run. Sequencing was performed on the NovaSeq 6000 system (Illumina) with a 150 bp paired-end protocol in Dynasty Gene Co. (Shanghai) and aligned to GRCh37/hg19 genome reference. The GATK toolkit (version 4.0.4.0) (McKenna et al., 2010) was then used to call the variants from the aligned BAM files. The results were annotated by SNPeff (Cingolani et al., 2012) and ANNOVAR (Wang et al., 2010) and deposited in variant calling format (VCF).

2.2 | Isolation of osteoblasts

Osteoblasts were isolated from the right femur of proband 1 (10 y/o, male), the right femur of proband 3 (4 y/o, female), left tibia and femur from two OI type IV patients with *COL1A2* frameshift and splice-site variants respectively (*COL1A2* c.3237_3238ins CGAGGCCCT CAGGGTCAC, p.I1079delinsIRGPQGH, 16 y/o, male; *COL1A2* c.792 + 1G- > T, splicing, 16 y/o, male), the right thumb of two individuals with polydactyly (2 y/o, female; 11 y/o, male). In brief, available skeletal tissues discarded after the operation were washed with PBS and digested with TrypLE Express (GIBCO) to remove all the soft tissues and blood cells. The calcified bones were cut into small pieces and immersed in the culture medium containing aMEM (GIBCO), 10% fetal bovine serum (GIBCO), penicillin (100 U/ml) and streptomycin (100 μg/ml) (GIBCO) for 1 ~ 2 weeks.

2.3 | RNA isolation, reverse-transcription PCR and quantitative PCR

Osteoblasts were lysed with Trizol (Thermo Fisher Scientific) and total RNA was isolated according to the manufacturer's instructions. Total RNA was used to generate cDNA from each sample by reverse transcription using Revert Aid First Strand cDNA Synthesis Kit (Thermo, K1622) and random hexamers. PCR was performed with *FKBP10* primers spanning the splice-site variant and the products were sent for Sanger sequencing (Sangon Biotech, Shanghai). Quantitative PCR was performed to compare the expression levels of selected genes using a Sybr-Green master mixture (Thermo, A25742).

Primer sequences used in this study are listed below:

Gene	Forward	Reverse	Size(bp)
FKBP10 NM_021939.4	CTGGTCTTTCACGTCCTCCT	R1: ATGATGTAACCCTGCCCGAT	215
		R2: CATTGCAGGTCTCAGATGGC	427
GAPDH NG_007073.2	GAAGGTGAAGGTCGGAGTC	GAAGATGGTGATGGGATTTC	226
BMP4 NG_009215.1	GCCAGCATGTCAGGATTAGC	AATCCAGTCATTCCAGCCCA	233
MMP13 NG_021404.1	AACGCCAGACAAATGTGACC	AGGTCATGAGAAGGGTGCTC	198
MEF2C NG_023427.1	TGGTTTCCGTAGCAACTCCT	TAGTGCAAGCTCCCAACTGA	228
RUNX2 NG_008020.2	CCAAATTTGCCTAACCAGAA	GCTCGATTGCAATTGTCTCT	335
SPP1 NG_030362.1	TGAAACGAGTCAGCTGGATG	TGAAATTCATGGCTGTGGAA	162

2.4 | Immunofluorescent staining

Immunofluorescent staining was performed as previously described (Stickens et al., 2004). Slides were dewaxed and rehydrated before blocking with blocking buffer (5% donkey serum (Jackson ImmunoResearch), 0.1% Triton X-100 (Sigma) in PBS) for 1 h. Cells with 80% confluency were washed with PBS and fixed in 4% paraformaldehyde for 15 min before blocking in a blocking buffer for 1 h. Samples were incubated with primary antibodies (anti-FKBP65, 1:500, Proteintech 12,172-1-AP; anti-SP7, 1:500, Abcam ab22552) overnight at 4°C, and detected with Alexa Fluor 488 secondary antibody (1:500, donkey anti-rabbit, Thermo Fisher Scientific) and mounting-medium with DAPI (Vector Laboratories). The signal was visualized with Zeiss inverted fluorescent microscope.

2.5 | Bone histology

The specimens were fixed in 4% paraformaldehyde and decalcified with 0.5 M EDTA before embedding in paraffin. 6 μm sections were cut and mounted on glass slides. The rehydrated sections were stained with Goldner's trichrome and visualized with a Leica DM3000 microscope.

2.6 | Bulk RNA sequencing

The isolated osteoblasts were lysed with Trizol (Thermo Fisher Scientific) and total RNA was extracted according to the manufacturer's instruction. RNA concentration was measured by Qubit and RNA integrity was assessed using the Agilent 2100. A total amount of 2 μg RNA per sample was used as input material. Sequencing libraries were generated using VAHTS mRNA-seq v2 Library Prep Kit for Illumina following the manufacturer's recommendations and sequenced on an Illumina NovaSeq platform to generate 150 bp paired-end reads by a commercial partner (Berry Genomics, Beijing). All primary sequencing data were deposited on the NCBI GEO website (GSE180838).

2.7 | Bioinformatic analyses of RNA sequencing data

Raw data (raw reads) of fastq format were first processed through primary quality control. Clean data were aligned to the reference human genome (GRCh38/hg38) and gene expression (FPKM values) was calculated for each transcript using the HISAT2 and Cufflinks package. (Kim et al., 2015; Trapnell et al., 2012) HTSeq package sequencing read count was calculated as described (Anders et al., 2015). Differential expression analysis between two conditions was performed using the cuffdiff tool in the Cufflink package. Differentially expressed genes were defined with adjusted p-value < .05 and the log2(Fold change) > 1. Genes with average values <1 in both groups under comparisons were excluded. GO (gene ontology) and KEGG pathway enrichment analysis of differentially expressed genes were performed on the DAVID website (Huang et al., 2007). GO terms with adjusted p-value < .05 were considered significantly enriched.

2.8 | Statistics

Data were presented as averages with standard deviation. Statistical significance level was evaluated by student's

t-test (two-tailed, unpaired) between two groups. The difference with $p < .05$ was considered to be significant.

3 | RESULTS

3.1 | Clinical features of patients with *FKBP10* variants

A cohort of 187 patients with low bone mass, frequent fracture and limb deformity was recruited in 2017 and 2021 in our hospital (Chen et al., 2022). To delineate the underlying genetic basis, genomic DNA from the peripheral blood was sent for targeted amplicon sequencing, covering all the exons and exon-intron boundaries in 24 genes associated with OI (see Materials and Methods). Amongst the cohort sequencing, we identified six patients (three children and three adults) harbouring biallelic variants in *FKBP10*.

The pedigree from a consanguineous Chinese family was shown in Figure 1a. A homozygous variant in the fifth intron of *FKBP10* (c.918-3C > G) was identified in the three children (proband 1–3). Dentinogenesis imperfecta was observed, whilst they had normal sclerae, hearing ability and intelligence (Figure 1b,c). Joint contracture or hypermobility associated with Bruck syndrome was not found. Frequent fractures were recorded more than five times, mainly in the lower extremities. The serum calcium, phosphate and alkaline phosphatase (ALP) levels were within normal range. Bone mineral density was significantly reduced, as indicated by Z scores (Table 1). Proband 1 did not have any treatment before visiting, whilst both probands 2 and 3 had received bisphosphonate treatment (Zoledronic acid). Proband 1 showed severe scoliosis (Cobb angle: 66°) and kyphoscoliosis with vertebral compression (Figure 1d). Probands 2 and 3 also displayed early onset of scoliosis (Figure 1e,f). The progressive spinal deformity was observed according to the Cobb angles measured in 2020 and 2021, respectively (Table 1).

Another three patients harbouring biallelic variants of *FKBP10* (proband 4: c. 745 C > T, p.Gln249*, c.825dupC, p.Gly278Argfs*95, compound heterozygous; proband 5: c.825dupC, p.Gly278Argfs*95, homozygous; proband 6: c.343C > T, p.Arg115*, homozygous) were also diagnosed with OI, showing low bone mass, limb deformity and abnormal spinal curvature (Table 1). Proband 4 showed mild scoliosis and kyphoscoliosis (Figure 1g). Proband 5 and proband 6 also showed severe scoliosis with a cobb angle >60° (Figure 1h,i).

3.2 | Variant identified in intron 5 of *FKBP10* leads to abnormal mRNA splicing

According to the OI variant database (https://www.le.ac.uk/genetics/collagen/, last update: 20 May 2020), ClinVar and PubMed literature, the variants (c.745C > T, p.Gln249* and c.825dupC, p.Gly278Argfs*95) had not been reported previously. Although the variant in the intron of *FKBP10* (c.918-3C > G) has been mentioned in several studies (Li et al., 2020; Xu et al., 2017), a detailed mechanistic study is still lacking. To test whether the variant in the splice acceptor site may affect the splicing of *FKBP10* mRNA, we extracted total RNA from the osteoblasts isolated from the probands and control individual and amplified the affected regions for analyses. Using primers flanking different regions from exon 5–7, we observed distinct mRNA isoforms with exon skipping and intron retention in the patient samples (Figure 2a). PCR with primer set 1 (F + R1) generated longer fragments in the patients than the control product, suggesting intron retention. Whilst PCR with primer set 2 (F + R2) generated a shorter major band in the patients, suggesting exon skipping. It was noteworthy that some minor larger bands from the PCR product of primer pair 2 were also observed, which may be resulted from the intron retention. To further confirm the PCR results, the amplified products were analyzed by Sanger sequencing. The sequencing results showed the c.918-3C > G variant caused the retention of intron 5 and deletion of exon 6 in the *FKBP10* mRNA isoforms of both patients (Figure 2b). To characterize the consequence of aberrant RNA splicing, we checked whether the protein translation was affected in these mutant osteoblasts. Surprisingly, no FKBP65 protein could be detected in the mutant osteoblasts, as compared to the control cells (Figure 2c). These data suggest that the variant identified in the intron acceptor site of *FKBP10* leads to abnormal mRNA splicing and truncated FKBP65 protein.

FIGURE 1 Clinical characteristics of patients with *FKBP10* variants. (a) The pedigree of the proband 1–3 and their family members. Filled-in symbols and half-filled-in symbols represent individuals with homozygous and heterozygous variants of *FKBP10* respectively. (b, c) Images from proband 3 showing dentinogenesis imperfecta and normal sclerae. (d-f) Frontal view of radiographs showing scoliosis in proband 1 (male, 10 y/o), proband 2 (female, 4 y/o) and proband 3 (female, 4 y/o). (g-i) Frontal view of radiographs from proband 4 (female, 24 y/o) with compound heterozygous variants (c.745C > T, p.Gln249* and c.825dupC, p.Gly278Argfs*95); proband 5 (female, 16 y/o) with homozygous variant (c.825dupC, p.Gly278Argfs*95); proband 6 (female, 32 y/o) with homozygous variant (c.343C > T, p.Arg115*) in *FKBP10*

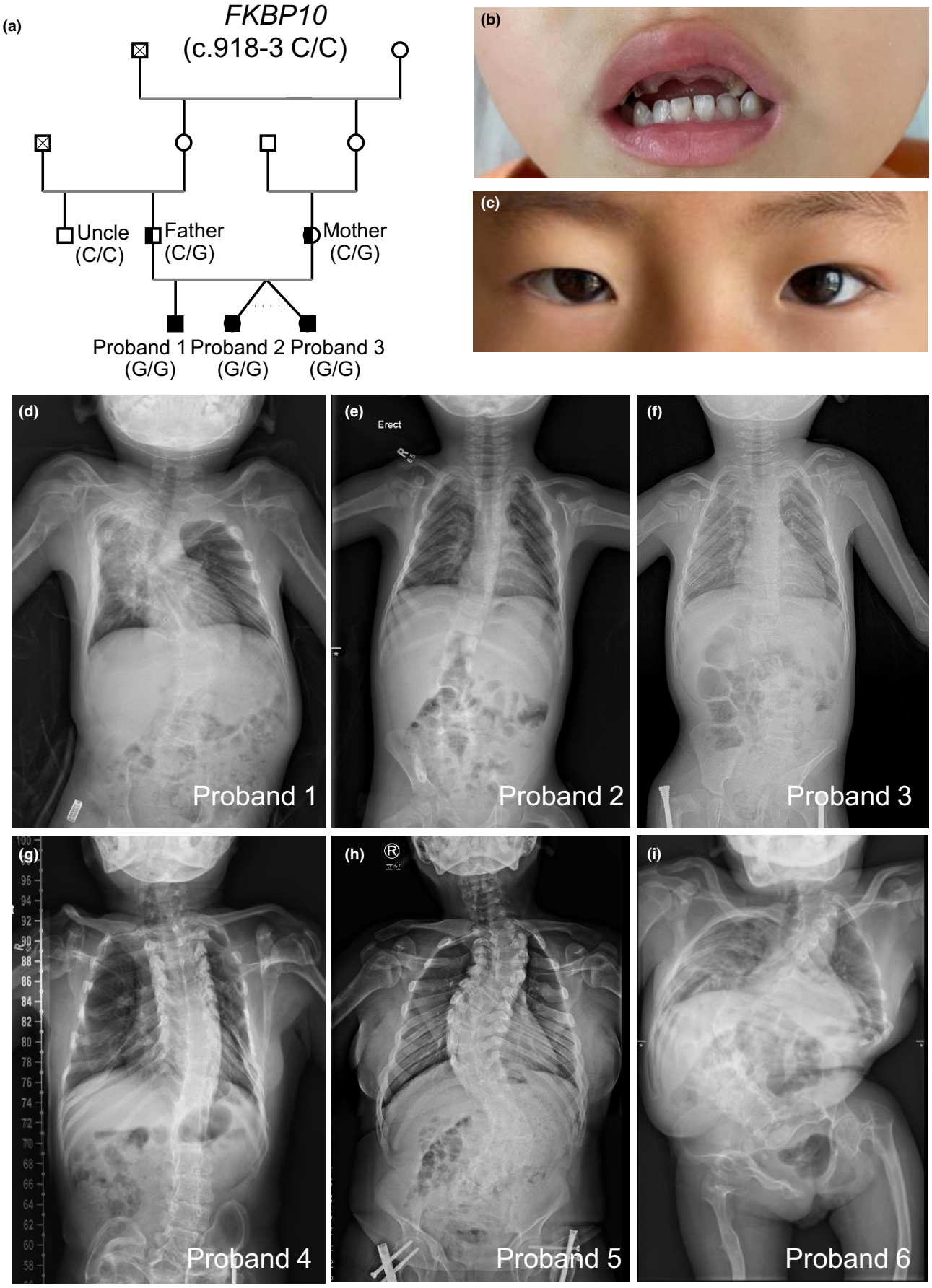
(a)
FKBP10
(c.918-3 C/C)
Uncle
(C/C)
Father
(C/G)
Mother
(C/G)
Proband 1
(G/G)
Proband 2
(G/G)
Proband 3
(G/G)
(b)
(c)
(d)
Proband 1
(e)
Erect
Proband 2
(f)
Proband 3
(g)
Proband 4
(h)
Proband 5
(i)
Proband 6

TABLE 1 Clinical characteristics

	Proband 1	Proband 2	Proband 3
FKBP10 variants	c.918-3C > G, homozygous	c.918-3C > G, homozygous	c.918-3C > G, homozygous
Age	10 y/o	4 y/o	4 y/o
Height / Weight	112 cm/18.6 kg	94 cm/13 kg	94 cm/13 kg
Blue sclera	–	–	–
Dentinogenesis imperfecta	+	+	+
Hearing loss	–	–	–
Joint contracture	–	–	–
Age of 1st fracture	At birth	1 month	2 y/o
Fracture times	10+	9	5
Serum Calcium (mmol/L)	N/A	2.5	2.4
Serum phosphate (mmol/L)	N/A	1.71	1.5
Serum ALP (ug/L)	N/A	228	208
Bisphosphonate treatment	–	Zoledronic acid	Zoledronic acid
LS BMD (g/cm^2) (Z score)	0.243 (−6.1)	0.349 (−2.5)	0.353 (−2.5)
Scoliosis/ Kyphoscoliosis	+	+	+
Cobb angle	66° (Mar 2021)	16° (Jul 2020) 24° (Mar 2021)	19° (Jul 2020) 30° (Mar 2021)

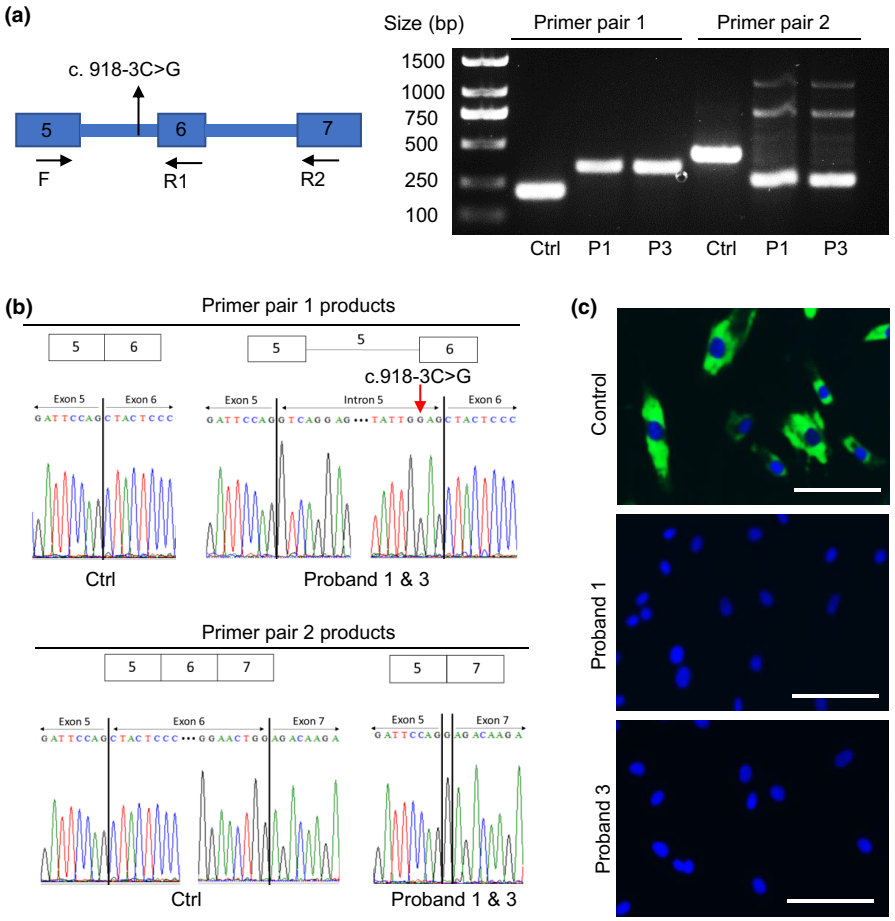

FIGURE 2 Genetic analysis and splicing effects caused by *FKBP10* variant (c.918-3C > G). (a) Gel electrophoresis separates PCR products using primer pairs spanning the splice-site variant (c.918-3C > G) of *FKBP10*. (b) Sanger sequencing results of the amplified PCR products. (c) Immunostaining of FKBP65 (green) on human primary osteoblasts isolated from control individual, proband 1 and 3 with DAPI (blue) counterstaining. Osteoblasts isolated from the right iliac biopsy of a patient with cerebral palsy (male, 27 y/o) were used as control here. Scale bar = 100 μm

Proband 4	Proband 5	Proband 6	Remarks
c.745C > T, p.Gln249*; c.825dupC, p.Gly278Argfs*95	c.825dupC, p.Gly278Argfs*95, homozygous	c.343C > T, p.Arg115*, homozygous	
26 y/o	16 y/o	32 y/o	
119 cm/36 kg	138 cm / 51 kg	98 cm/30 kg	
–	–	–	Rare
+	–	–	Rare
–	–	–	Rare
+	+	–	Bruck syndrome
1 y/o	1 y/o	4 y/o	
5	10+	10+	
N/A	2.43	N/A	2.13–2.70
N/A	1.41	N/A	1.29–2.26 (child)
N/A	125	94	42–390 (child)
–	Zoledronic acid	–	
0.847 (−1.8)	0.964 (−0.2)	0.619(−4.2)	
+	+	+	
25° (Dec 2020)	71° (Jun 2021)	120° (Sep 2017)	

3.3 | Loss of *FKBP10* leads to abnormal bone morphology and collagen alignment

FKBP65 plays a crucial role in the post-translational modification of type I procollagen telopeptides. To understand the underlying pathogenesis of OI caused by loss of FKBP65, we further characterized the bone geometrical property in the control and affected individuals. From a mechanical perspective, the strength of bone is determined not only by the degree of mineralization but even more importantly by the arrangement of collagen fibres (Viguet-Carrin et al., 2006). Bone histology from the normal skeletal sample (fracture humerus, 13 y/o, male) demonstrated a condensed and organized lamellar pattern (Figure 3a,e), whilst bones from patients with *FKBP10* variants were porous with disorganized collagen alignment (Figure 3b–d, f–h). Transaxial sections indicated that the sizes of haversian canals and resorption cavities were significantly increased in the cortical bones from proband 1, proband 2 and proband 4, when compared to control samples showing compact haversian structure (Figure 3i–l). Thus, the increasing porosity in the cortical bones of *FKBP10* patients resulted in abnormal bone geometry, reduced mechanical toughness and skeletal deformity.

FKBP65 is crucial for the lysine hydroxylation in the C-terminal telopeptide and prevents premature aggregation of type I procollagen. To test whether the collagen processing was affected without FKBP65, we stained type I collagen in the osteoblasts isolated from *FKBP10* probands and control individuals. The amount of type I collagen detected in the intracellular compartment was much higher in the mutant cells compared with the control (Figure 3m–o), suggesting collagen processing defects with loss of *FKBP10*.

3.4 | Loss of *FKBP10* results in aberrant osteoblast differentiation

Removal of *Fkbp10* specifically in osteoblasts results in altered collagen crosslinking, qualitative defect in the skeleton and impaired biomechanical strength in mice (Lietman et al., 2017). To further characterize the roles of *FKBP10* in osteoblast differentiation and maturation, we isolated osteoblasts from probands 1 and 2 and generated transcriptomic data to delineate the impact of FKBP65 at the transcriptional level (Table S1, sheet 1). Principal component analysis (PCA) indicated that cells with similar genotypes ($FKBP10^{LoF}$, $COL1^{OI}$ and non-OI control osteoblasts) were clustered together (Figure 4a). When comparing data across different clusters, we found 1571 differentially expressed genes (DEGs) between $FKBP10^{LoF}$ and control osteoblasts, and only 460 DEGs between $FKBP10^{LoF}$ and $COL1^{OI}$ groups, suggesting that defects of *FKBP10* and type I collagen have a similar impact on osteoblast differentiation (Figure 4b–d, Table S1, sheet 2–4). The expression of *FKBP10* was significantly downregulated both in probands 1 and 2, confirming the splice-site

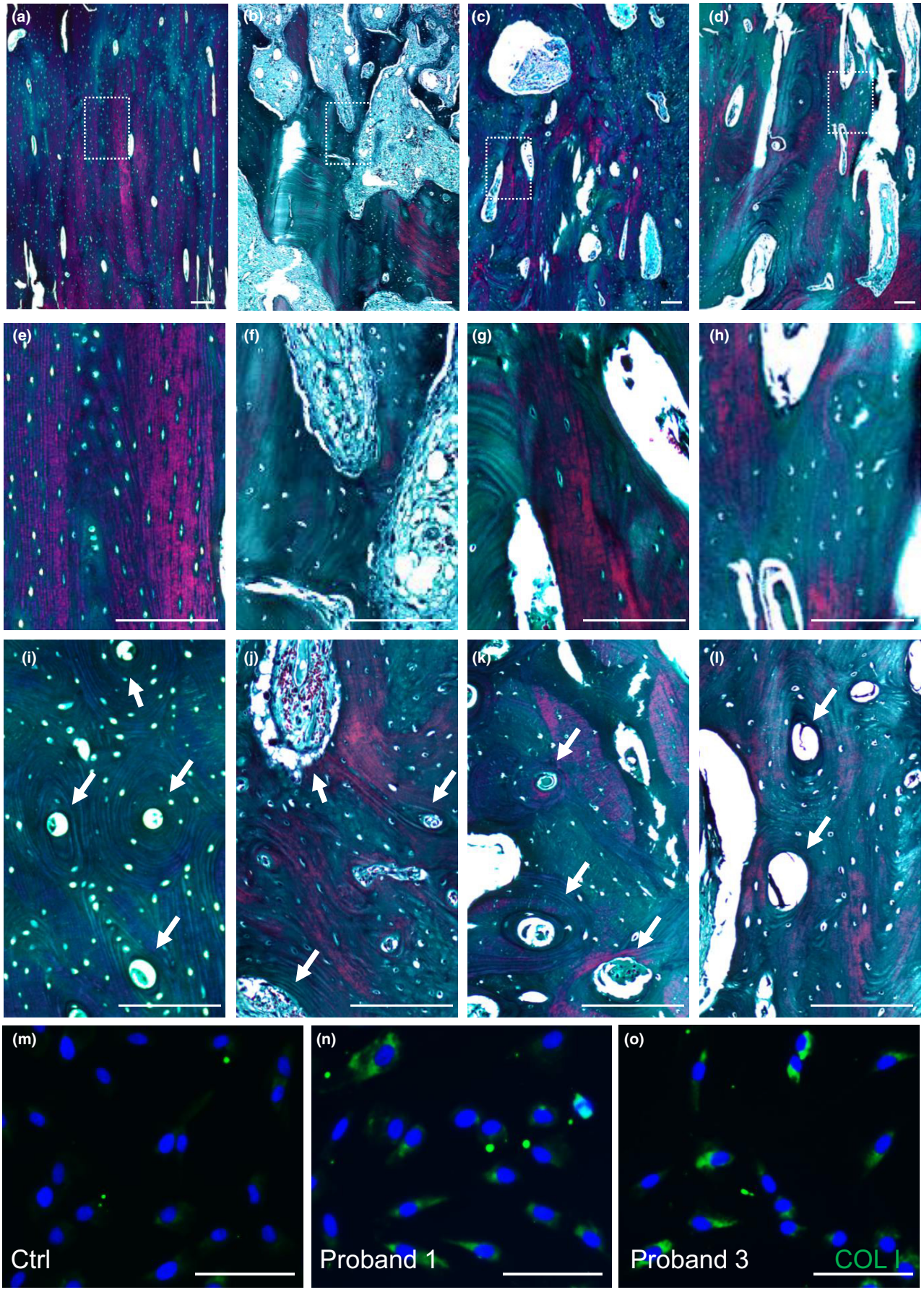
(a)
(b)
(c)
(d)
(e)
(f)
(g)
(h)
(i)
(j)
(k)
(l)
(m)
(n)
(o)
Ctrl
Proband 1
Proband 3
COL I

variant in the intron 5 affected the maturation of *FKBP10* mRNA. The common DEGs were displayed by heatmap (Figure 4e).

To identify the enriched biological processes affected by the loss of *FKBP10*, we performed Gene Ontology enrichment analysis using DEGs commonly changed in different comparisons. Genes associated with biology process of 'cell adhesion', 'extracellular matrix organization', 'regulation of osteoblast differentiation', 'positive regulation of PI3K signalling' and 'positive regulation of BMP signalling pathway' were enriched in those common DEGs (Figure 4f, Table S2), revealing that collagen processing, organization and osteoblast differentiation were defective in *FKBP10* mutated patients. In the common DEGs, *BMP4* and *TGFB2* were specifically downregulated in $FKBP10^{LoF}$ osteoblasts, whilst *NOG* (BMP antagonist) was upregulated (Figure 4e).

The porous structure has been observed in the bones of the probands (Figure 3), consistent with a high bone turnover rate in OI patients (Braga et al., 2004). From the transcriptomic analysis, we found the expression of *ALPL* (encoding Alkaline Phosphatase) was significantly increased in all OI samples as compared to the control group (Figure 4b,c). To confirm, we measured the bone alkaline phosphatase activity in osteoblasts. Consistently, the ALP activities were higher in the osteoblasts from *FKBP10* patients when compared to control cells (Figure 5a). Increased turnover rate may contribute to the abnormal bone structure in OI patients.

To gain deeper insight into the abnormal osteoblast differentiation, we found the expression of transcription factors crucial for skeletal development, including *RUNX2, MEF2C, BMP4, MMP13* and *SPP1*, were significantly downregulated in $FKBP10^{LoF}$ and $COL1^{OI}$ osteoblasts, implying common cellular pathogenesis in OI patients (Figure 5b, Table S1, sheet 2). Quantitative real-time PCR validated the downregulation trends of these osteogenic markers in the proband osteoblasts (Figure 5c). SP7 is an osteoblast-specific transcription factor that plays crucial role during the differentiation of immature osteoblasts into functional osteoblasts and osteocytes (Baek & Kim, 2011; Nakashima et al., 2002). Staining of SP7 indicated that the expression level of SP7 and the numbers of expressing skeletal cells were dramatically reduced in *FKBP10* probands as compared to the fracture control sample (Figure 5d–g).

4 | DISCUSSION

Our study reported six OI patients caused by autosomal recessive variants of *FKBP10*. Two of the variants (c.745C > T and c.825dupC) have not been reported previously. We also revealed the impact of c.918-3C > G variant on the *FKBP10* mRNA splicing. Both intron retention and exon skipping were observed. It was suggested that distinct mRNA isoforms were generated due to the presence of donor/acceptor site variants, the order of intron removal and the use of cryptic splicing sites (Takahara et al., 2002; Wang et al., 2016). These patients were characterized by osteopenia, frequent fractures and progressive spinal deformity (scoliosis and kyphoscoliosis). Scoliosis has been reported as a phenotypic feature of type XI OI (Kelley et al., 2011; Li et al., 2020; Umair et al., 2016; Xu et al., 2017). Scoliosis is a complex three-dimensional deformity of the spine, whilst its aetiology and pathogenesis remain unclear. A range of hypotheses has been proposed to explain the pathogenesis of scoliosis, including genetics, skeletal spinal growth and bone metabolism, metabolic pathways, biomechanics and the central nervous system (Cheng et al., 2015). However, none of these parameters has been conclusively shown to be a causative factor for scoliosis development. The prevalence of scoliosis was higher in more severe OI (type III: 89%, type IV: 61%) than in mild form of OI (type I: 36%) (Sato et al., 2016). The recessive form of OI often displays more severe clinical features (Li et al., 2020), suggesting that variants causing a severe form of OI could be considered a risk factor for scoliosis. In our study, the three children developed early onset of scoliosis, which is defined by Cobb angle ≥10° by the age of 10 (El-Hawary & Akbarnia, 2015; Skaggs et al., 2014; Williams et al., 2014).

The newly formed triple helix of type I collagen is stabilized by chaperones HSP47 and FKBP65. Further modifications including hydroxylation occur during transport from the ER to the Golgi apparatus. Any disturbance can lead to the activation of unfolded protein response (UPR) and ER-associated degradation pathway (Marini et al., 2017). From the cellular staining, we observed that the secretion of type I collagen was arrested in the *FKBP10* mutant cells (Figure 3m–o). However, at the transcriptional level, we did not detect activation of ER stress and UPR in the $FKBP10^{LoF}$ osteoblasts. The expression of *DDIT3*, *BiP* and *ATF3*, essential markers

FIGURE 3 Analyses of bone histology and collagen processing. (a-l) Goldner trichrome staining of skeletal samples from a control individual (a, e, i), proband 1 (b, f, j), proband 3 (c, g, k) and proband 4 (d, h, l). Collagen matrix alignment was shown by sagittal sections (a-d) with boxed regions shown in higher magnification in (e-h). The haversian structure was shown by transaxial sections (i-l). (m-o) Immunostaining of type I collagen (COL I) in the primary osteoblasts (green) from control individual (m), proband 1 (n) and proband 3 (o). A skeletal sample from a healthy individual with a right humerus fracture (male, 14 y/o) was used as control here. Scale bars = 200 μm

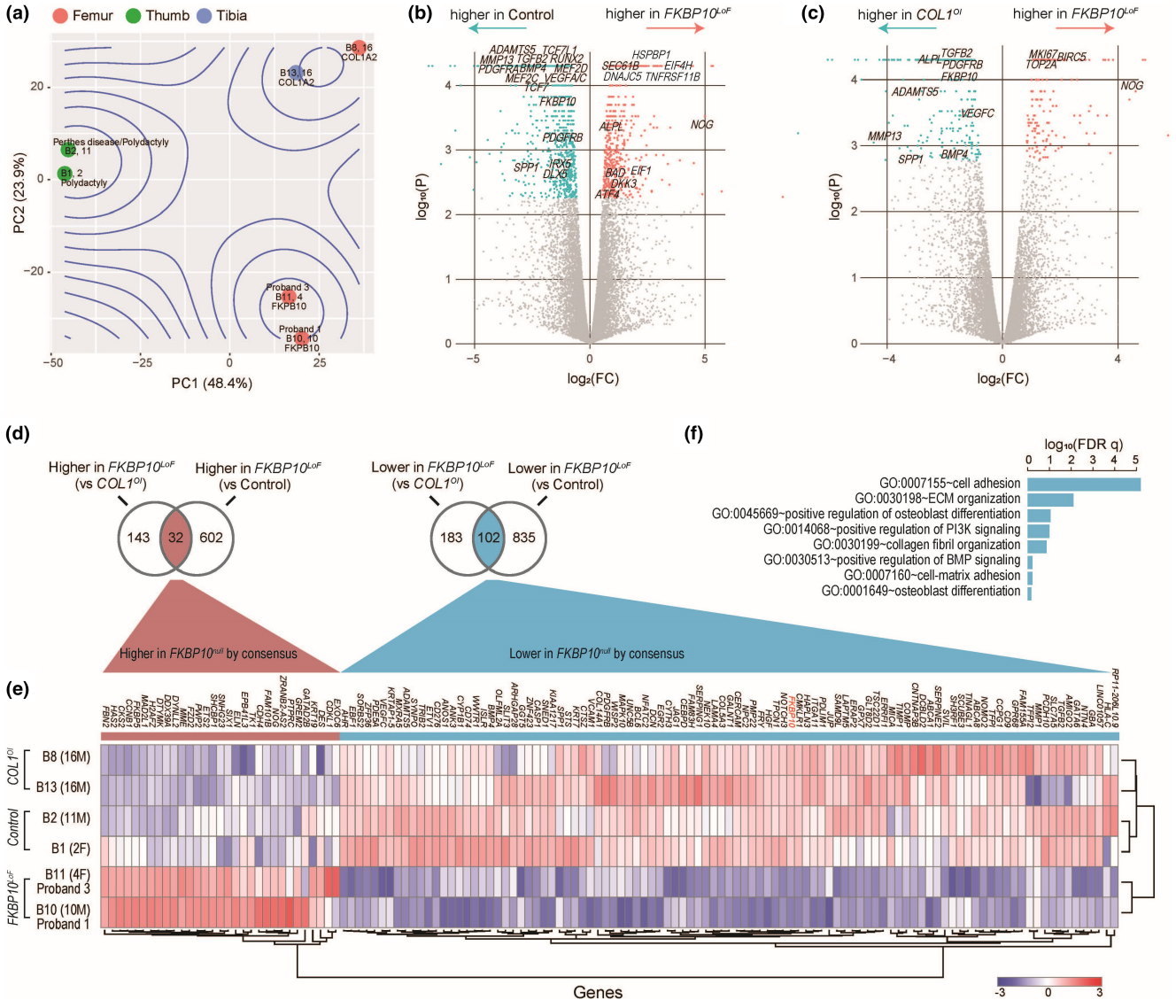

FIGURE 4 Transcriptomic analyses. (a) Principal component analysis (PCA) shows the overall correlation of the 6 transcriptomic samples. Percentages in brackets indicated a fraction of the total data variances explained. Blue curves were density contours. (b) Volcano plot showing the differentially expressed genes (DEGs) between the *FKBP10*^{LoF} group and the control group. (c) Volcano plot showing the DEGs between the *FKBP10*^{LoF} group and the *COL1*^{OI} group. (d-e) Venn diagrams and heatmap showing the DEGs consistently up and downregulated in *FKBP10*^{LoF} group as compared with the other two groups. (f) Bar chart showing representative gene ontology (GO) terms of the 102 genes downregulated in the *FKBP10*^{LoF} group. Transcriptomic data of osteoblasts isolated from the right thumbs of two individuals with polydactyly (male, 11 y/o; female, 2 y/o) were used as control here

for UPR activation (Oyadomari & Mori, 2004), was not significantly deviated from control cells (Table S1, sheet 3), whilst the genes involved in the ER-associated degradation and Golgi transportation were significantly upregulated in *FKBP10*^{LoF} cells (Figure S1a), consistent with the important role of FKBP65 during procollagen processing from the ER to Golgi.

From the histological analysis, we found abnormal bone morphology and cell distribution in the OI patients. By comparing the transcriptomic data, we further confirmed that the expression levels of crucial regulators (*RUNX2, MEF2C* and *DLX5*) for osteoblast differentiation were significantly downregulated in *FKBP10* patients, providing a sign of abnormal osteoblast activity. Pathway enrichment analysis indicated that genes involved in BMP/TGF-β were enriched in the DEGs (*BMP4*, *TGFB2* and *NOG*). BMP and TGF-β signalling pathways have fundamental roles in skeletal development and bone homeostasis. Dysregulated BMP and TGF-β signalling result in a number of bone disorders in humans. BMPs and TGF-β transduce signals through canonical SMAD-dependent and non-canonical MAPK pathways to regulate *Runx2* and other downstream mediators to promote osteoblast differentiation (Wu et al., 2016). The genetic effect of

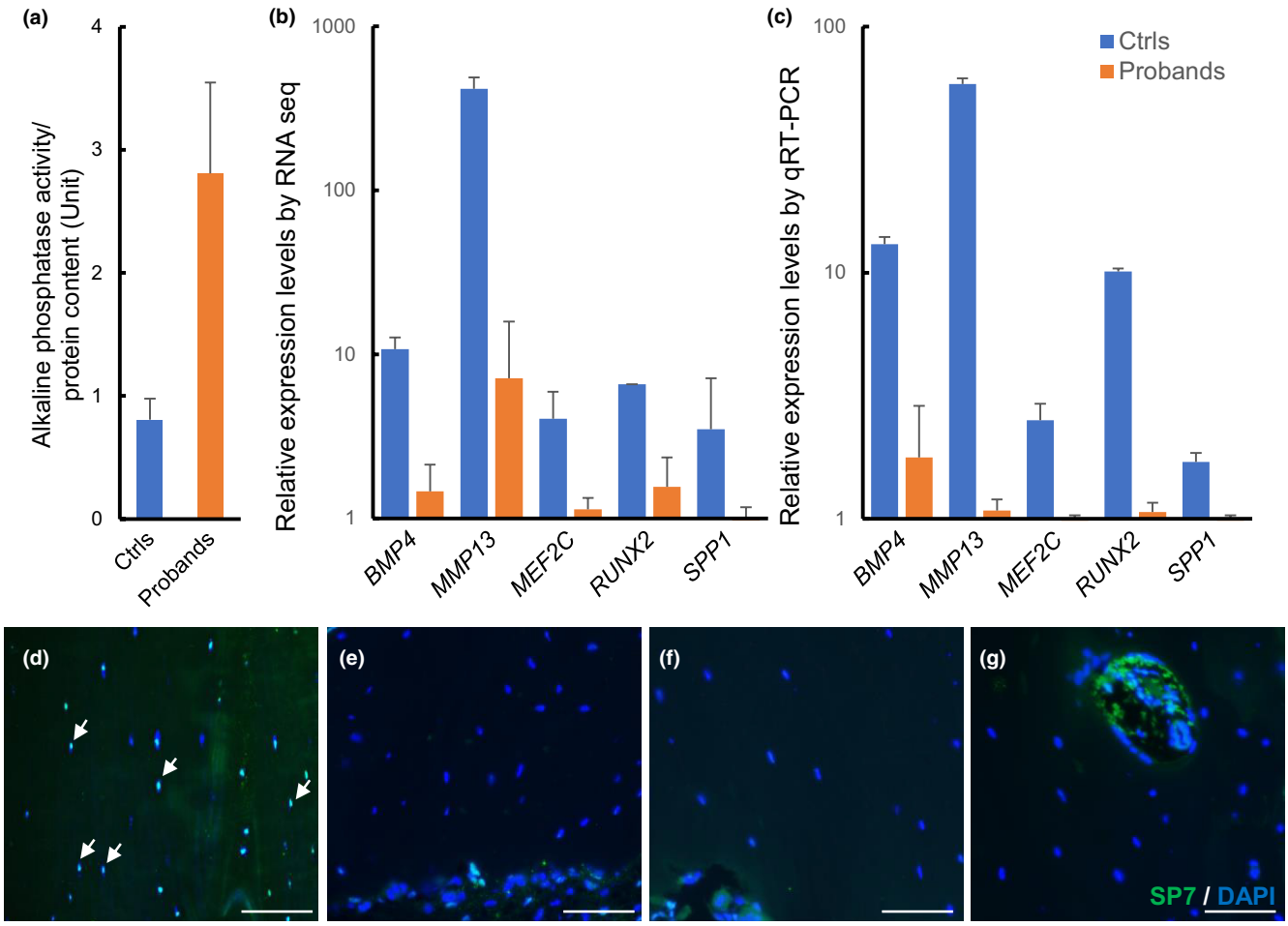

FIGURE 5 Disrupted osteoblast differentiation with *FKBP10* loss-of-function. (a) Alkaline phosphatase (ALP) activities from primary osteoblasts isolated from *FKBP10* probands and control individuals. The activity was expressed as mean-SD. Osteoblasts isolated from the right thumbs of two individuals with polydactyly (male, 11 y/o; female, 2 y/o) were used as control here. (b, c) expression changes of osteogenic markers in osteoblasts from *FKBP10* probands compared to control individuals by bulk RNA sequencing and quantitative real-time PCR. The expression level of each gene from proband 3 was set as 1, and the levels from proband 1 and control individuals were normalized with the same magnification fold change. The expression was expressed as mean-SD ($n = 2$). mRNA from osteoblasts isolated from the right thumbs of two individuals with polydactyly (male, 11 y/o; female, 2 y/o) was used as control here. (d-g) Immuno-staining of SP7 on the skeletal sections from fracture control (d), proband 1 (e), proband 3 (f) and proband 4 (g). A skeletal sample from a healthy individual with a right humerus fracture (male, 14 y/o) was used as control here. Scale bar = 100 μm

polymorphisms in the promoter regions of *BMP4*, *Leptin* and *MMP3* have been found to be synergistic for susceptibility to scoliosis (Morocz et al., 2011). Cellular studies of primary osteoblasts from scoliosis patients have shown abnormal gene expression and osteogenic differentiation potential (Zhang et al., 2018). Mutations disrupting other pathways such as NOTCH signalling have also been found to cause human congenital scoliosis. Molecules involved in the NOTCH pathway (*NOTCH3* and *JAG1*) were down-regulated in the patient osteoblasts (Table S1, sheet 3). Further investigation is warranted to study the underlying transcriptional network associated with the deformed spine in scoliosis.

Evidence showed that bisphosphonates could improve bone mass and reduce long bone deformity in OI, which had been widely used as an antiresorptive treatment to improve BMD and Z score for OI patients (Kashii et al., 2019; Sato et al., 2016). However, retrospective analyses of scoliosis in children with OI showed limited effects of bisphosphonates on lowering the incident of developing scoliosis at maturity (Marini et al., 2017; Ward et al., 2011). This is in accordance with our records. Probands 2 and 3 received Zoledronic acid treatment. However, their Cobb angle rose from 16° to 24° and 19° to 30°, respectively (Table 1). Although bisphosphonates may not reduce the prevalence of scoliosis, the treatment can decrease the progression rate in type III OI patients, and the relief of vertebral compression enabled the use of pedicular screws and clamps to give stronger fixation for spinal deformity operations (Sato et al., 2016).

In summary, our study described the clinical features of six OI patients with *FKBP10* mutations. The homozygous variant identified in the fifth intron of *FKBP10* (c.918-3C>G) led to abnormal RNA processing and loss of FKBP65 protein. The histological and transcriptomic analyses helped to gain insight into the function of FKBP65 in collagen processing and osteoblast differentiation. Further investigation may be needed for a comprehensive understanding of the roles of *FKBP10* during skeletal development and spinal homeostasis.

AUTHOR CONTRIBUTIONS

ZT, HTS, PC and MT conceived and designed the research studies. MT, ZD, YZ and SY provided diagnoses and performed surgeries on the patients. AQ and LD provided nursing care and documented the clinical data. ZT and HTS conducted the experiments and acquired the data. PC conducted bioinformatics analyses. ZT, HTS, PC and MT analysed the data. ZT, HTS and MT wrote the original manuscript. BG helped with genetic diagnosis, data interpretation and manuscript editing. MT acquired research funding and supervised the study. All authors revised and approved the manuscript.

ACKNOWLEDGEMENTS

This work was supported by Shenzhen "Key Medical Discipline Construction Fund" (No. SZXK077), Guangdong Provincial Basic and Applied Research Fund (2022A1515010987), Shenzhen Sanming Project (SZSM201612055) and Hong Kong Health and Medical Research Fund (No. 07181676). We thank the Fu Tak Iam Foundation (Hong Kong) and Chow Tai Fook charity foundation (Hong Kong) for covering part of the medical costs. ZT (20210802658C) and PKC (20210830100C) are supported by the Shenzhen Peacock Plan.

CONFLICT OF INTEREST

The authors declare that they have no competing interests.

ETHICS STATEMENT

This study was approved by the Institutional Review Broad of University of Hong Kong—Shenzhen Hospital ([2016]08 and [2020]190). Detailed medical history and physical examination were assessed and collected by clinicians. Peripheral blood was obtained from available family members for a genetic test. Available skeletal tissues discarded after the operation were collected for osteoblast isolation. Informed consent was obtained for all patients and their family members.

DATA AVAILABILITY STATEMENT

All primary sequencing data were deposited on the NCBI GEO website (GSE180838) (MATERIALS AND METHODS 2.6). For the missing data, we will provide the original data upon request.

REFERENCES

Alanay, Y., Avaygan, H., Camacho, N., Utine, G. E., Boduroglu, K., Aktas, D., Alikasifoglu, M., Tuncbilek, E., Orhan, D., Bakar, F. T., Zabel, B., Superti-Furga, A., Bruckner-Tuderman, L., Curry, C. J. R., Pyott, S., Byers, P. H., Eyre, D. R., Baldridge, D., Lee, B., … Krakow, D. (2010). Mutations in the gene encoding the RER protein FKBP65 cause autosomal-recessive osteogenesis imperfecta. *American Journal of Human Genetics*, *86*(4), 551–559. https://doi.org/10.1016/j.ajhg.2010.02.022

Anders, S., Pyl, P. T., & Huber, W. (2015). HTSeq--a python framework to work with high-throughput sequencing data. *Bioinformatics*, *31*(2), 166–169. https://doi.org/10.1093/bioinformatics/btu638

Baek, W. Y., & Kim, J. E. (2011). Transcriptional regulation of bone formation. *Frontiers in Bioscience (Scholar Edition)*, *3*, 126–135. https://doi.org/10.2741/s138

Barnes, A. M., Duncan, G., Weis, M., Paton, W., Cabral, W. A., Mertz, E. L., Makareeva, E., Gambello, M. J., Lacbawan, F. L., Leikin, S., Fertala, A., Eyre, D. R., Bale, S. J., & Marini, J. C. (2013). Kuskokwim syndrome, a recessive congenital contracture disorder, extends the phenotype of FKBP10 mutations. *Human Mutation*, *34*(9), 1279–1288. https://doi.org/10.1002/humu.22362

Braga, V., Gatti, D., Rossini, M., Colapietro, F., Battaglia, E., Viapiana, O., & Adami, S. (2004). Bone turnover markers in patients with osteogenesis imperfecta. *Bone*, *34*(6), 1013–1016. https://doi.org/10.1016/j.bone.2004.02.023

Bybee, S. M., Bracken-Grissom, H., Haynes, B. D., Hermansen, R. A., Byers, R. L., Clement, M. J., Udall, J. A., Wilcox, E. R., & Crandall, K. A. (2011). Targeted amplicon sequencing (TAS): A scalable next-gen approach to multilocus, multitaxa phylogenetics. *Genome Biology and Evolution*, *3*, 1312–1323. https://doi.org/10.1093/gbe/evr106

Chen, P., Tan, Z., Shek, H. T., Zhang, J. N., Zhou, Y., Yin, S., Dong, Z., Xu, J., Qiu, A., Dong, L., Gao, B., & To, M. K. T. (2022). Phenotypic Spectrum and molecular basis in a Chinese cohort of osteogenesis imperfecta with mutations in type I collagen. *Frontiers in Genetics*, *13*, 816078. https://doi.org/10.3389/fgene.2022.816078

Cheng, J. C., Castelein, R. M., Chu, W. C., Danielsson, A. J., Dobbs, M. B., Grivas, T. B., Gurnett, C. A., Luk, K. D., Moreau, A., Newton, P. O., Stokes, I. A., Weinstein, S. L., & Burwell, R. G. (2015). Adolescent idiopathic scoliosis. *Nature Reviews. Disease Primers*, *1*, 15030. https://doi.org/10.1038/nrdp.2015.30

Cingolani, P., Platts, A., Wang le, L., Coon, M., Nguyen, T., Wang, L., Land, S. J., Lu, X., & Ruden, D. M. (2012). A program for annotating and predicting the effects of single nucleotide polymorphisms, SnpEff: SNPs in the genome of Drosophila melanogaster strain w1118; iso-2; iso-3. *Fly (Austin)*, *6*(2), 80–92. https://doi.org/10.4161/fly.19695

El-Hawary, R., & Akbarnia, B. A. (2015). Early onset scoliosis - time for consensus. *Spinal Deformity*, *3*(2), 105–106. https://doi.org/10.1016/j.jspd.2015.01.003

Forlino, A., Cabral, W. A., Barnes, A. M., & Marini, J. C. (2011). New perspectives on osteogenesis imperfecta. *Nature Reviews. Endocrinology*, *7*(9), 540–557. https://doi.org/10.1038/nrendo.2011.81

Huang, D. W., Sherman, B. T., Tan, Q., Collins, J. R., Alvord, W. G., Roayaei, J., Stephens, R., Baseler, M. W., Lane, H. C., & Lempicki, R. A. (2007). The DAVID gene functional classification tool: A novel biological module-centric algorithm to functionally analyze large gene lists. *Genome Biology*, *8*(9), R183. https://doi.org/10.1186/gb-2007-8-9-r183

Ishikawa, Y., Vranka, J., Wirz, J., Nagata, K., & Bachinger, H. P. (2008). The rough endoplasmic reticulum-resident FK506-binding protein FKBP65 is a molecular chaperone that interacts with collagens. *The Journal of Biological Chemistry*, *283*(46), 31584–31590. https://doi.org/10.1074/jbc.M802535200

Kashii, M., Kanayama, S., Kitaoka, T., Makino, T., Kaito, T., Iwasaki, M., Kubota, T., Yamamoto, T., Ozono, K., & Yoshikawa, H. (2019). Development of scoliosis in young children with osteogenesis imperfecta undergoing intravenous bisphosphonate therapy. *Journal of Bone and Mineral Metabolism*, *37*(3), 545–553. https://doi.org/10.1007/s00774-018-0952-x

Kelley, B. P., Malfait, F., Bonafe, L., Baldridge, D., Homan, E., Symoens, S., Willaert, A., Elcioglu, N., Van Maldergem, L., Verellen-Dumoulin, C., Gillerot, Y., Napierala, D., Krakow, D., Beighton, P., Superti-Furga, A., De Paepe, A., & Lee, B. (2011). Mutations in FKBP10 cause recessive osteogenesis imperfecta and Bruck syndrome. *Journal of Bone and Mineral Research*, *26*(3), 666–672. https://doi.org/10.1002/jbmr.250

Kim, D., Langmead, B., & Salzberg, S. L. (2015). HISAT: A fast spliced aligner with low memory requirements. *Nature Methods*, *12*(4), 357–360. https://doi.org/10.1038/nmeth.3317

Li, S., Cao, Y., Wang, H., Li, L., Ren, X., Mi, H., Wang, Y., Guan, Y., Zhao, F., Mao, B., Yang, T., You, Y., Guan, X., Yang, Y., Zhang, X., & Zhao, X. (2020). Genotypic and phenotypic analysis in Chinese cohort with autosomal recessive osteogenesis imperfecta. *Frontiers in Genetics*, *11*, 984. https://doi.org/10.3389/fgene.2020.00984

Lietman, C. D., Lim, J., Grafe, I., Chen, Y., Ding, H., Bi, X., Ambrose, C. G., Fratzl-Zelman, N., Roschger, P., Klaushofer, K., Wagermaier, W., Schmidt, I., Fratzl, P., Rai, J., Weis, M. A., Eyre, D., Keene, D. R., Krakow, D., & Lee, B. H. (2017). Fkbp10 deletion in osteoblasts leads to qualitative defects in bone. *Journal of Bone and Mineral Research*, *32*(6), 1354–1367. https://doi.org/10.1002/jbmr.3108

Marini, J. C., Forlino, A., Bachinger, H. P., Bishop, N. J., Byers, P. H., Paepe, A., Fassier, F., Fratzl-Zelman, N., Kozloff, K. M., Krakow, D., Montpetit, K., & Semler, O. (2017). Osteogenesis imperfecta. *Nature Reviews Disease Primers*, *3*, 17052. https://doi.org/10.1038/nrdp.2017.52

McKenna, A., Hanna, M., Banks, E., Sivachenko, A., Cibulskis, K., Kernytsky, A., Garimella, K., Altshuler, D., Gabriel, S., Daly, M., & DePristo, M. A. (2010). The genome analysis toolkit: A MapReduce framework for analyzing next-generation DNA sequencing data. *Genome Research*, *20*(9), 1297–1303. https://doi.org/10.1101/gr.107524.110

Moosa, S., Yamamoto, G. L., Garbes, L., Keupp, K., Beleza-Meireles, A., Moreno, C. A., Valadares, E. R., de Sousa, S. B., Maia, S., Saraiva, J., Honjo, R. S., Kim, C. A., Cabral de Menezes, H., Lausch, E., Lorini, P. V., Lamounier, A., Jr., TCB, C., Giunta, C., Rohrbach, M., ... Netzer, C. (2019). Autosomal-recessive mutations in MESD cause osteogenesis imperfecta. *American Journal of Human Genetics*, *105*(4), 836–843. https://doi.org/10.1016/j.ajhg.2019.08.008

Morocz, M., Czibula, A., Grozer, Z. B., Szecsenyi, A., Almos, P. Z., Rasko, I., & Illes, T. (2011). Association study of BMP4, IL6, leptin, MMP3, and MTNR1B gene promoter polymorphisms and adolescent idiopathic scoliosis. *Spine (Phila Pa 1976)*, *36*(2), E123–E130. https://doi.org/10.1097/BRS.0b013e318a511b0e

Nakashima, K., Zhou, X., Kunkel, G., Zhang, Z., Deng, J. M., Behringer, R. R., & de Crombrugghe, B. (2002). The novel zinc finger-containing transcription factor osterix is required for osteoblast differentiation and bone formation. *Cell*, *108*(1), 17–29. https://doi.org/10.1016/s0092-8674(01)00622-5

Oyadomari, S., & Mori, M. (2004). Roles of CHOP/GADD153 in endoplasmic reticulum stress. *Cell Death and Differentiation*, *11*(4), 381–389. https://doi.org/10.1038/sj.cdd.4401373

Sato, A., Ouellet, J., Muneta, T., Glorieux, F. H., & Rauch, F. (2016). Scoliosis in osteogenesis imperfecta caused by COL1A1/COL1A2 mutations - genotype-phenotype correlations and effect of bisphosphonate treatment. *Bone*, *86*, 53–57. https://doi.org/10.1016/j.bone.2016.02.018

Satoh, M., Hirayoshi, K., Yokota, S., Hosokawa, N., & Nagata, K. (1996). Intracellular interaction of collagen-specific stress protein HSP47 with newly synthesized procollagen. *The Journal of Cell Biology*, *133*(2), 469–483. https://doi.org/10.1083/jcb.133.2.469

Skaggs, D. L., Akbarnia, B. A., Flynn, J. M., Myung, K. S., Sponseller, P. D., Vitale, M. G., Chest Wall and Spine Deformity Study Group; Growing Spine Study Group, Pediatric Orthopaedic Society of North America, & Scoliosis Research Society Growing Spine Study, C. (2014). A classification of growth friendly spine implants. *Journal of Pediatric Orthopedics*, *34*(3), 260–274. https://doi.org/10.1097/BPO.0000000000000073

Stickens, D., Behonick, D. J., Ortega, N., Heyer, B., Hartenstein, B., Yu, Y., Fosang, A. J., Schorpp-Kistner, M., Angel, P., & Werb, Z. (2004). Altered endochondral bone development in matrix metalloproteinase 13-deficient mice. *Development*, *131*(23), 5883–5895. https://doi.org/10.1242/dev.01461

Takahara, K., Schwarze, U., Imamura, Y., Hoffman, G. G., Toriello, H., Smith, L. T., Byers, P. H., & Greenspan, D. S. (2002). Order of intron removal influences multiple splice outcomes, including a two-exon skip, in a COL5A1 acceptor-site mutation that results in abnormal pro-alpha1(V) N-propeptides and Ehlers-Danlos syndrome type I. *American Journal of Human Genetics*, *71*(3), 451–465. https://doi.org/10.1086/342099

Trapnell, C., Roberts, A., Goff, L., Pertea, G., Kim, D., Kelley, D. R., Pimentel, H., Salzberg, S. L., Rinn, J. L., & Pachter, L. (2012). Differential gene and transcript expression analysis of RNA-seq experiments with TopHat and cufflinks. *Nature Protocols*, *7*(3), 562–578. https://doi.org/10.1038/nprot.2012.016

Umair, M., Hassan, A., Jan, A., Ahmad, F., Imran, M., Samman, M. I., Basit, S., & Ahmad, W. (2016). Homozygous sequence variants in the FKBP10 gene underlie osteogenesis imperfecta in consanguineous families. *Journal of Human Genetics*, *61*(3), 207–213. https://doi.org/10.1038/jhg.2015.129

van Dijk, F. S., Semler, O., Etich, J., Kohler, A., Jimenez-Estrada, J. A., Bravenboer, N., Claeys, L., Riesebos, E., Gegic, S., Piersma, S. R., Jimenez, C. R., Waisfisz, Q., Flores, C.-L., Nevado, J., Harsevoort, A. J., Janus, G. J. M., Franken, A. A. M., van der Sar, A. M., Meijers-Heijboer, H., ... Micha, D. (2020). Interaction between KDELR2 and HSP47 as a key determinant in osteogenesis imperfecta caused by Bi-allelic variants in KDELR2.

American Journal of Human Genetics, *107*(5), 989–999. https://doi.org/10.1016/j.ajhg.2020.09.009

Viguet-Carrin, S., Garnero, P., & Delmas, P. D. (2006). The role of collagen in bone strength. *Osteoporosis International*, *17*(3), 319–336. https://doi.org/10.1007/s00198-005-2035-9

Wang, K., Li, M., & Hakonarson, H. (2010). ANNOVAR: Functional annotation of genetic variants from high-throughput sequencing data. *Nucleic Acids Research*, *38*(16), e164. https://doi.org/10.1093/nar/gkq603

Wang, Z., Iida, A., Miyake, N., Nishiguchi, K. M., Fujita, K., Nakazawa, T., Alswaid, A., Albalwi, M. A., Kim, O. H., Cho, T. J., Lim, G. Y., Isidor, B., David, A., Rustad, C. F., Merckoll, E., Westvik, J., Stattin, E. L., Grigelioniene, G., Kou, I., … Ikegawa, S. (2016). Axial Spondylometaphyseal dysplasia is caused by C21orf2 mutations. *PLoS One*, *11*(3), e0150555. https://doi.org/10.1371/journal.pone.0150555

Ward, L. M., Rauch, F., Whyte, M. P., D'Astous, J., Gates, P. E., Grogan, D., Lester, E. L., McCall, R. E., Pressly, T. A., Sanders, J. O., Smith, P. A., Steiner, R. D., Sullivan, E., Tyerman, G., Smith-Wright, D. L., Verbruggen, N., Heyden, N., Lombardi, A., & Glorieux, F. H. (2011). Alendronate for the treatment of pediatric osteogenesis imperfecta: A randomized placebo-controlled study. *The Journal of Clinical Endocrinology and Metabolism*, *96*(2), 355–364. https://doi.org/10.1210/jc.2010-0636

Williams, B. A., Matsumoto, H., McCalla, D. J., Akbarnia, B. A., Blakemore, L. C., Betz, R. R., Flynn, J. M., Johnston, C. E., McCarthy, R. E., Roye, D. P., Jr., Skaggs, D. L., Smith, J. T., Snyder, B. D., Sponseller, P. D., Sturm, P. F., Thompson, G. H., Yazici, M., & Vitale, M. G. (2014). Development and initial validation of the classification of early-onset scoliosis (C-EOS). *The Journal of Bone and Joint Surgery. American Volume*, *96*(16), 1359–1367. https://doi.org/10.2106/JBJS.M.00253

Wu, M., Chen, G., & Li, Y. P. (2016). TGF-beta and BMP signaling in osteoblast, skeletal development, and bone formation, homeostasis and disease. *Bone Research*, *4*, 16009. https://doi.org/10.1038/boneres.2016.9

Xu, X. J., Lv, F., Liu, Y., Wang, J. Y., Ma, D. D., Asan, Wang, J. W., Song, L. J., Jiang, Y., Wang, O., Xia, W. B., Xing, X. P., & Li, M. (2017). Novel mutations in FKBP10 in Chinese patients with osteogenesis imperfecta and their treatment with zoledronic acid. *Journal of Human Genetics*, *62*(2), 205–211. https://doi.org/10.1038/jhg.2016.109

Zhang, J., Chen, H., Leung, R. K. K., Choy, K. W., Lam, T. P., Ng, B. K. W., Qiu, Y., Feng, J. Q., Cheng, J. C. Y., & Lee, W. Y. W. (2018). Aberrant miR-145-5p/beta-catenin signal impairs osteocyte function in adolescent idiopathic scoliosis. *The FASEB Journal*, *32*(12), fj201800281. https://doi.org/10.1096/fj.201800281

SUPPORTING INFORMATION

Additional supporting information can be found online in the Supporting Information section at the end of this article.

How to cite this article: Tan, Z., Shek, H. T., Chen, P., Dong, Z., Zhou, Y., Yin, S., Qiu, A., Dong, L., Gao, B., & To, M. K. T. (2023). Clinical features and molecular characterization of Chinese patients with *FKBP10* variants. *Molecular Genetics & Genomic Medicine*, *11*, e2122. https://doi.org/10.1002/mgg3.2122